

Spontaneous chirality via long-range electrostatic forces

Kevin L. Kohlstedt,¹ Francisco Solis,² Graziano Vernizzi,¹ and Monica Olvera de la Cruz¹

¹*Department of Materials Science, Northwestern University, Evanston, Illinois 60208*

²*Department of Integrated Natural Sciences, Arizona State University, Glendale, Arizona 85306*

(Dated: October 28, 2018)

We consider a model for periodic patterns of charges constrained over a cylindrical surface. In particular we focus on patterns of chiral helices, achiral rings or vertical lamellae, with the constraint of global electroneutrality. We study the dependence of the patterns' size and pitch angle on the radius of the cylinder and salt concentration. We obtain a phase diagram by using numerical and analytic techniques. For pure Coulomb interactions, we find a ring phase for small radii and a chiral helical phase for large radii. At a critical salt concentration, the characteristic domain size diverges, resulting in macroscopic phase segregation of the components and restoring chiral symmetry. We discuss possible consequences and generalizations of our model.

PACS numbers: 05.70.Np, 41.20.Cv, 64.60.Cn, 82.70.Uv

The ubiquitous role electrostatics play in the organization of biomolecular assemblies is a main pillar of modern biophysics (see, for instance, [1] and references therein). The co-assembly of oppositely charged molecules [2] often occurs over cylindrical structures with directional dependent functionalities, such as in fibers or filamentous viruses [2, 3] for signal transmission or cellular structure mobility [4]. Other important cationic-anionic cylindrical co-assemblies include actin-binding proteins structures [5], cylindrical micelles [6], and peptide-amphiphile fibers [7, 8]. A considerable aspect of these systems is the presence of surface charge heterogeneities or domains [9, 10], which arises from the competition of electrostatic forces with segregating forces such as steric, van der Waals, and hydrogen bonding interactions. These surface patterns have been shown to be important for the stability and functionality of the aggregates [2, 11, 12, 13].

A key feature in many biological processes is pattern recognition and specificity within isomeric aggregates [14]. Biomolecules exploit repetitive patterning over surfaces, which often breaks some underlying symmetry, in order to increase their functionality [15]. In this context, chiral symmetry (that is the absence of improper rotation axis) is notably interesting: although its role in chemistry and biology is widely recognized [2, 16, 17, 18], its origin in biology is the subject of much debate [19]. Many systems are chiral due to the chirality of its components [19, 20]. For instance, colloidal solutions of rod-like viruses provide an intriguing example of chiral structures in liquid crystalline phases [21]. Nevertheless, understanding whether electrostatic interactions alone are capable of producing chiral systems would shed further light on the issue.

From a theoretical vantage point, the electrostatic patterning of a system of charges on cylindrical surfaces is however relatively unexplored. Certainly, the effects of long-range electrostatic forces have been widely studied for planar two dimensional systems [22]; also the behavior of short-range interactions over cylindrical geometries

has been addressed, such as the Ising model on the cylinder [23]. We analyze here an intermediate case where charges are confined over a cylindrical surface and interact via long-range forces. A further issue we consider is whether spherically symmetric electrostatic interactions are capable to break translational, rotational or chiral isometries of the cylinder. Recently, there has been interest to study crystalline systems over constrained geometries such as the surface of spheres, cylinders, and tori [24, 25, 26]. The generalization to more general curved substrates shows an interesting rich behavior [27].

In this Letter we provide the full phase diagram of lamellar charged patterns on a cylinder, as a function of the cylinder radius and screening length. We explicitly show the existence of a phase where the system spontaneously adopts chiral configurations. We study also its "Coulombic" origin by observing how it disappears when increasing the screening length. Our model is a generalization of the one introduced by F.J. Solis et al. [9] for charge domains on cylindrical cationic-anionic co-assemblies in aqueous solution. We consider a 1:1 stoichiometric mixture that covers the surface completely. The surface can generally be considered incompressible due to the strength of hydrophobic interactions. The degree of the incompatibility among the cationic and anionic components – characterized by the standard Flory-Huggins parameter χ – drives the molecules to separate and minimize the interfacial energy between the positive and negative surface groups. While χ leads the system to segregation, the long-range Coulomb potential favors mixing. Molecules of like charge form homogeneous domains of average charge density σ ; boundaries between such domains acquire a line tension γ . In the strongly segregated limit we assume the lowest-energy configuration corresponds to domains arranged on a periodic lattice $\{\mathbf{A}\}$. This system can be described by a coarse-grained two-terms free energy $\mathcal{F} = \mathcal{F}_1 + \mathcal{F}_2$ of a Wigner-Seitz cell, with the line tension term \mathcal{F}_1 opposing the

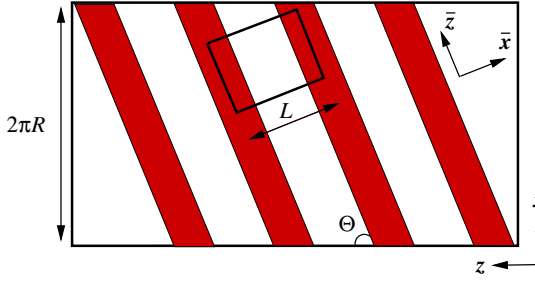


FIG. 1: Schematic view of an unwrapped cylinder with a generic helical pattern, showing the notation used in the text.

surface charge density term \mathcal{F}_2 [9]:

$$\mathcal{F}_1 = \gamma l, \quad \mathcal{F}_2 = \frac{1}{2} \iint' d^2\mathbf{x} d^2\mathbf{y} \sigma(\mathbf{x}) U(\mathbf{x}-\mathbf{y}) \sigma(\mathbf{y}), \quad (1)$$

where l is the interfacial length between the domains, $\sigma(\mathbf{x})$ is the local charge density, and \iint' represents an integration over the whole surface and the other restricted to a single Wigner-Seitz unit cell. In real systems the electrostatic potential is attenuated by free ions in the solvent and we adopt a screened Coulomb potential:

$$U(\mathbf{x}) = \frac{1}{4\pi\epsilon} \frac{e^{-\kappa|\mathbf{x}|}}{|\mathbf{x}|}, \quad (2)$$

where ϵ is the dielectric constant, and κ is the inverse Debye-Hückle length. The latter takes effectively into account possible salt concentration in the solution, and we will use it here also as a tunable parameter to control the long-range/short-range nature of the interactions. The two terms in the free energy \mathcal{F} generate a characteristic length $L_0 = \sqrt{\gamma\epsilon}/\sigma$, and it is therefore convenient to adopt dimensionless units. All lengths x are measured in units of L_0 , $\tilde{x} = x/L_0$, $\tilde{l} = l/L_0$, the inverse screening length becomes $\tilde{\kappa} = \kappa L_0$, the charge density $\tilde{\sigma} = \sigma/L_0^2$, and the free energy is measured in units of $\mathcal{F}_0 = \gamma L_0$, i.e. $\tilde{\mathcal{F}} = \mathcal{F}/\mathcal{F}_0$. For the sake of compactness in the rest of this Letter we assume that the name of a variable stands for its dimensionless counterpart, and we drop all the tilde symbols. We consider the free energy density $F = \mathcal{F}/A_c$, where A_c is the area of the Wigner-Seitz cell. A self-consistent minimization of the free energy F for a planar system gives lamellar patterns at 1:1 stoichiometric ratio [9], and it has been confirmed by direct numerical simulations [28]. Henceforth we concentrate on the behavior of such lamellar patterns and their critical properties on the cylinder. In that case, we have $F_1 = 2/L$ where L is the distance between two neighboring lamellae [9]. The double integral in F_2 can be computed first by “unwrapping” the surface of the cylinder of radius R onto an infinite set of parallel stripes of size $2\pi R$ on the plane, and then by summing all the pairwise electrostatic interactions over the planar periodic lattice $\{\mathbf{\Lambda}\}$ of the lamellae, by Fourier decomposition method. To simplify the calculations we

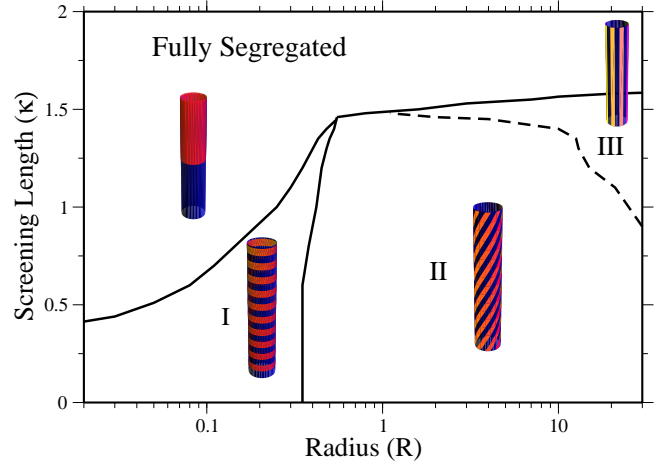


FIG. 2: Phase diagram of our model. Region I is the ring phase; Region II is the helical phase; Region III is the axial phase; the region at the top is the fully segregated phase. The solid lines are discontinuous transitions and the dashed line is a continuous crossover.

adopted a square lattice oriented along the lamellae (see Fig. 1). Formally:

$$F_2 = \frac{1}{2} \sum_{\mathbf{\Lambda}} \int_{cell} d\xi \int_{cell} d\eta \sigma(\xi) \sigma(\mathbf{\Lambda} + \eta) V(\mathbf{\Lambda} + \eta - \xi), \quad (3)$$

where

$$V(\mathbf{p}) = \frac{e^{-\kappa D}}{4\pi D} \theta(2\pi R - |p_x|), \quad (4)$$

with $D \equiv \sqrt{4R^2 \sin^2(p_x/(2R)) + p_z^2}$ is the projected distance of $\mathbf{p} \equiv (p_x, p_z)$ on the $\{x, z\}$ plane, and $\theta(x)$ is the step function. By introducing the reciprocal lattice $\{\mathbf{Q}\}$, defined by $\mathbf{Q} \cdot \mathbf{\Lambda} = 2\pi m$, $m \in \mathbb{Z}$, and by using the Poisson summation formula we have:

$$F_2 = \frac{1}{2A_c} \sum_{\mathbf{Q}} \hat{\sigma}(\mathbf{Q}) \hat{\sigma}(-\mathbf{Q}) \hat{V}(\mathbf{Q}), \quad (5)$$

where $\hat{\sigma}(\mathbf{Q})$ and $\hat{V}(\mathbf{Q})$ are the Fourier transforms of σ and V , respectively. They are:

$$\hat{V}(\mathbf{Q}) = R I_{q_x R}(\xi) K_{q_x R}(\xi), \quad (6)$$

$$\hat{\sigma}(\mathbf{Q}) = 4 \frac{\sin(\bar{q}_x/4)}{\bar{q}_x} \delta(\bar{q}_z), \quad (7)$$

where $\xi \equiv R\sqrt{\kappa^2 + q_z^2}$ and I_ν and K_ν are modified Bessel functions of order ν of the first kind and second kind, respectively. For simplicity we used the twofold notation $\mathbf{Q} = (\bar{q}_x, \bar{q}_z)$ in the reference system parallel to the lamellar domains, and $\mathbf{Q} = (q_x, q_z)$ in the reference system parallel to the axis of the cylinder (see Fig. 1). Let Θ be the pitch angle between the axis of the cylinder z and the direction of the lamellar stripes \bar{z} . Any lattice on

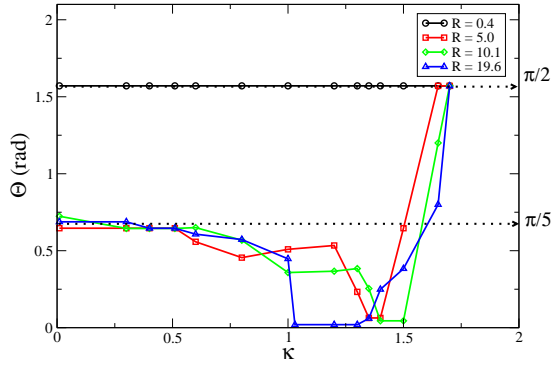


FIG. 3: Evolution of the pitch angle Θ of helical lamellae with the Debye screening inverse-length κ , at different cylinder radii R .

the surface of a cylinder must be commensurate with its circumference, that is it must be periodic in the x direction with period $2\pi R$. The commensurability constraint in the reciprocal space read $\bar{q}_x = 2\pi m/L$ or equivalently $q_x = 2\pi m \cos \Theta/L$ and $q_z = 2\pi m \sin \Theta/L$, $m \in \mathbb{Z}$. Moreover $q_x R = mn$ must hold, where n is the number of lamellar stripes per pitch.

We numerically minimized the free energy density F with respect to all possible lamellar lattices, i.e. with respect to the spacing L and the pitch angle Θ for several values of R and κ . Our results are collected in the phase diagram in Fig. 2. There are four regions: a phase **I** characterized by ring patterns, a chiral phase **II** characterized by helical patterns, a phase **III** characterized by vertical lamellar patterns, and a fully segregated phase.

Phase **I** is limited to fibers with circumference smaller than the domain size. This is natural when considering the limit $R \ll L$ where $\cos \Theta \simeq nL/2\pi R \rightarrow 1$, i.e. $\Theta \simeq \pi/2$, which is precisely the observed ring phase.

Phase **II** is the primary result of this work. It proves the existence of chiral configurations (both right-handed and left-handed) due to electrostatic long-range interactions. A surprising feature of this phase is that at $\kappa = 0$ there is a preferred pitch angle $\Theta^* \simeq \pi/5$ (see Fig. 3). The long-range nature of electrostatic interaction may be the reason of such a preference, since by increasing $\kappa > 0$ the pitch angle decreases continuously down to the vertical lamellar phase **III**. Our numerical findings can be further justified on a theoretical ground by looking at the large- R asymptotic expansion of the free energy. In the expansion q_x is kept fixed while the density $\sigma(\mathbf{x})$ is not dependent on R since it is defined locally over a unit cell. For the potential $\hat{V}(\mathbf{Q})$ we obtain (up to $O(1/R^4)$ terms):

$$\hat{V}(\mathbf{Q}) \sim \frac{1}{2\sqrt{Q^2 + \kappa^2}} - \frac{(4Q^2 - 5q_z^2 - \kappa^2)(q_z^2 + \kappa^2)}{16(Q^2 + \kappa^2)^{7/2}} \frac{1}{R^2} \quad (8)$$

where $Q \equiv \sqrt{q_z^2 + q_x^2}$. The leading term is the planar

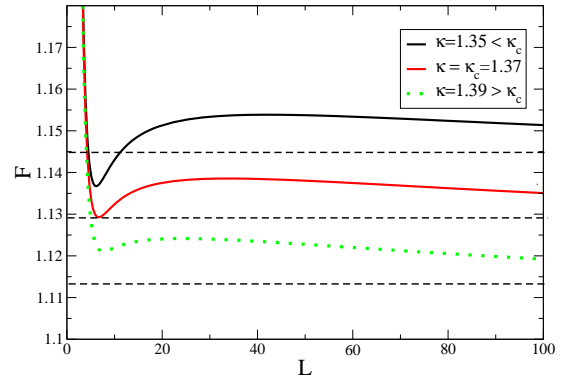


FIG. 4: By increasing the screening length above a critical value κ_c , the free energy global minimum jumps from a finite L to $L = \infty$. In this plot $R = 1000$ and $\kappa_c = 1.37 \pm 0.05$

limit studied in [28]. It is straightforward to show that the minimum of the free energy F at $\kappa = 0$ with respect to the pitch angle is where $d\hat{V}(\mathbf{Q})/d\Theta = 0$. From eq. (8) at $\kappa = 0$ we find $\Theta^* = \arccos \sqrt{3/5} \simeq 0.68$ rad which is close to the numerical value $\pi/5 \simeq 0.63$ rad. For $\kappa > 0$ the first-order correction to Θ^* is negative and scale as κ^2 . This is in agreement with the numerical behavior depicted in Fig. 3, that the pitch angle initially decreases when increasing κ . From eq. (8) we obtain also the value $\kappa_0 = 2\sqrt{2/3}\pi/L$ at which the pitch angle vanishes, i.e. where phase **II** merges continuously into **III** and the helical patterns evolve into vertical stripes. We find $L = 5.8 \pm 0.2$ at large- R (see Fig. 4), and therefore $\kappa_0 = 0.9 \pm 0.2$. The nature of phase **II** can further be seen in the discontinuous transition to the achiral phase **I**. Assuming the separation distance L is not strongly dependent on R , there is a critical ratio L/R such that, as R decreases, Θ discontinuously jumps from Θ^* to $\pi/2$ (see Fig. 3).

All the three phases we considered so far are bound at large κ by a fully-segregated phase. Such a salt-induced phase transition is a first-order phase transition as the free energy jumps from a finite cell size to an infinite cell size (see Fig. 4). Let $\kappa_c(R)$ be the critical value of κ at which this transition occurs. In Fig. 3 the transition is at the jump of the pitch to $\pi/2$, near the “melting” transition point $\kappa \sim \kappa_c$. At large- R we find $\kappa_c = 1.6 \pm 0.1$. The melting transition can be interpreted by a scaling argument. At large- L the free-energy scales as $F \approx 1/L + 1/\kappa$. If κ is small then the global minimum is at a finite value of L , that is the size of the Wigner cell (see continuous black line in Fig. 4). If κ is large then the minimum jumps to infinity, that is to a macroscopically segregated system (see dotted green line in Fig. 4).

We note that the phase diagram for the cylinder is richer than its planar counterpart. In fact, due to the commensurability constraints of the cylindrical surface new lamellar pattern configurations with different chiral angles arise for different radii R and lamellar spacing L .

The theoretical prediction for the cylindrical geometry in the large radius limit agrees well with the result for planar geometry. However a striking distinction from the planar case is the appearance of a preferred chiral angle of about $\Theta^* = \arccos \sqrt{3/5} \approx \pi/5$, which is numerically found to be conserved over a wide range of radii. It is an amusing coincidence this angle corresponds to the one found in recent studies of capsid-protein arrangements on cylindrical viruses [21] as well as in biomimetic self-organized nanotubes [2]. However Coulomb interaction is not in principle the driving force of the assemblies considered in [2, 21]. Therefore an interesting question is whether such a pitch angle is universal, and what is its origin. We attempt an answer by considering the large- R asymptotic expansion for higher-order decaying isotropic interactions, $V_3 \sim 1/D^3$. We find (up to $O(1/R^4)$ terms: $\hat{V}_3(\mathbf{Q}) \sim -\pi Q + \pi q_z^2/(8Q^5 R^2)$), whose stationary points are only at $\Theta = 0$ and $\pi/2$ (this statement holds true also for higher multipolar terms). Although this argument cannot be considered as proof, it shows that the universality of the pitch angle is unlikely. However it also shows that the $\sim \pi/5$ angle seems to arise in conjunction with the Coulomb potential. As we have seen, the exponential screening term actually softens this effect through the reduction of the pitch angle, but it does not suppress it entirely (for small values of κ). From this point of view, the chiral symmetry we observe originates only from the interplay between the $1/D$ behavior of the Coulomb potential and the cylindrical geometry. Such an effect is independent from the specific pattern σ and therefore we believe it might emerge also in more general electrostatic systems over a cylinder.

The symmetry group of a decorated cylinder falls into one of 9 classes, each with a distinct closed subgroup of the full cylinder group $\mathbf{SO}(2) \times \mathbb{R}$ [29]. The four regions in our diagram correspond to the four classes characterized by one-dimensional closed subgroups (the rest being zero- or two-dimensional). Namely, up to conjugacy and scaling, they are [29]: pure rotations $\mathbf{SO}(2) \times \mathbb{I}$ (fully segregated phase), continuous rotations and discrete translations $\mathbf{SO}(2) \times \mathbb{Z}$ (phase **I**), discrete rotations and continuous translations $\mathbf{Z}_k \times \mathbb{R}$ (phase **III**), and corkscrew symmetries $\mathbf{Z}_k \times \mathbf{L}$ (phase **II**). \mathbf{Z}_k is the subgroup of rotations of the cylinder through angles that are multiples of $2\pi/k$, and $\mathbf{L} = \{(t, t) \in \mathbf{SO}(2) \times \mathbb{R} : t \in \mathbb{R}\}$. Therefore the phase transitions we observe correspond to breaking qualitatively different symmetry generators.

We expect these phases to be relevant for systems at the nanoscale, as it can be easily seen by an order-of-magnitude analysis of L_0 . It is through these length scales we believe the functionality of the patterns might manifest, such as the induced chirality in our system. The advantage of the nanoscale, besides possible practical applications, is that electrostatic interactions are still important under normal dielectric conditions. Even in aqueous systems where charge screening occurs, Coulomb

interactions still play a vital role through counterions and metallic-ion coordination [30]. Finally, we do not explore in this Letter the possibility of a critical point where phase **I**, **II** or the fully segregated phase meet, and we postpone it to future studies.

The authors acknowledge Dr. Y. Velichko for useful discussions. This work was supported in part by the NSF (Grant No. DMR-0414446) and by a graduate fellowship of the DOE (Grant No. DE-FG02-97ER25308 for KLK).

-
- [1] Y. Levin, *Physica A* **352**, 43 (2005).
 - [2] F. Artzner, *PNAS* **100**, 981 (2003).
 - [3] M. Suzuki, A. Hirao, and A. Mizuno, *J. Biol. Chem.* **278**, 51448 (2003).
 - [4] D. Lehnert et al., *J. Cell Science* **117**, 41 (2004).
 - [5] B.N. Thomas et al., *J. Am. Chem. Soc.* **120**, 12178 (1998).
 - [6] E.W. Kaler et al., *J. Phys. Chem.* **96**, 6698 (1992).
 - [7] K.L. Niece et al., *J. Am. Chem. Soc.* **125**, 7146 (2003).
 - [8] G.A. Silva et al., *Science* **303**, 1352 (2004).
 - [9] F.J. Solis, S.I. Stupp, and M. Olvera de la Cruz, *J. Chem. Phys.* **122**, 054905 (2005).
 - [10] S.M. Loverde, F.J. Solis, and M. Olvera de la Cruz, To be published.
 - [11] F. Tombolato, A. Ferrarini, and E. Grelet, *Phys. Rev. Lett.* **96**, 258302 (2006).
 - [12] E.E. Meyer et al., *PNAS* **102**, 6839 (2005).
 - [13] Y.S. Velichko and M.O. de la Cruz, *Phys. Rev. E* **72**, 041920 (2005).
 - [14] S.Y. Qi, J.T. Groves, and A.K. Chakraborty, *PNAS* **98**, 6548 (2001).
 - [15] G. Vereb, et al., *PNAS* **100**, 8053 (2003).
 - [16] G.T. Pickett, M. Gross, and H. Okuyama, *Phys. Rev. Lett.* **85**, 3652 (2000).
 - [17] A.B. Harris, R.D. Kamien, and T.C. Lubensky, *Rev. Mod. Phys.* **71**, 1745 (1999).
 - [18] A.A. Kornyshev and S. Leikin, *Phys. Rev. Lett.* **84**, 2537 (2000).
 - [19] M.A. Mateos-Timoneda, M. Crego-Calama, and D.N. Reinhoudt, *Chem. Soc. Rev.* **33**, 363 (2004).
 - [20] A.A. Kornyshev, S. Leikin, and S.V. Malinin, *Eur. Phys. J. E* **7**, 83 (2002).
 - [21] E. Grelet and S. Fraden, *Phys. Rev. Lett.* **90**, 198302 (2003).
 - [22] U. Low, V.J. Emery, K. Fabricius and S.A. Kivelson, *Phys. Rev. Lett.* **72**, 1918 (1994).
 - [23] J.L. Cardy, *J. Phys. A* **17**, L385 (1984).
 - [24] M.J. Bowick, A. Cacciuto, D.R. Nelson, and A. Traveset, *Phys. Rev. B* **73**, 024115 (2006).
 - [25] H. Edlund, A. Sadaghiani, and A. Khan, *Langmuir* **13**, 4953 (1997).
 - [26] I. Endo and H. Koibuchi, *Phys. Lett. A* **350**, 11 (2006).
 - [27] V. Vitelli, J.B. Lucks, and D.R. Nelson, *PNAS* **103**, 12323 (2006).
 - [28] S.M. Loverde, Y.S. Velichko, and M. Olvera de la Cruz, *J. Chem. Phys.* **124**, 144702 (2006).
 - [29] M. Golubitsky and I. Melbourne, in *Proceedings of Bridges Conference*, 1998, R. Sarhangi ed., p. 209-223.
 - [30] J.M. Lehn, *Rep. Prog. Phys.* **67**, 249 (2004).